

# Photochemical stability of cellulose textile surfaces painted with some reactive azo-triazine dyes

Liliana Rosu · Dan Rosu · Cristian-Catalin Gavat ·  
Cristian-Dragos Varganici

Received: 9 October 2013 / Accepted: 4 March 2014 / Published online: 20 March 2014  
© Springer Science+Business Media New York 2014

**Abstract** The influence of ultraviolet irradiation of different doses ( $\lambda > 300$  nm) on the structural and color modifications of cotton fabrics painted with four different azo-triazine dyes (Reactive Yellow 143, Reactive Orange 13, Reactive Red 183, and Reactive Red 2) was studied. High irradiation doses up to  $3500 \text{ J cm}^{-2}$  led to changes in the dyes structures. Structural changes before and after the complete irradiation were compared by applying FTIR, UV-Vis, and near infrared chemical imaging techniques. Color modifications were also investigated. Color differences significantly increased with the irradiation dose for all the studied samples.

## Introduction

Although the skin protection against the ultraviolet (UV) radiation provided by textile fabrics has been a topic for some years, there still exists a lack of knowledge on the subject. It is wrongly believed that any textile article would be appropriate for UV protection. Natural fabrics such as cotton, silk, and wool provide a low skin protection due to the low absorption degree of UV radiation [1]. In fact, the protection provided by a garment depends on fiber type, structural characteristics, color and dyeing intensity, and the presence of optical brightening agents or UV absorbers

[2–8]. Most of the textiles remain colored throughout inside and outside and are exposed to varying doses of sunlight. Solar lights intensity is an important parameter of photochemical processes [9]. The color perception of dyed textiles is explained by the selective absorption at a certain wavelength of the incident visible light by the dyestuff molecules of the material surface. The unabsorbed wavelengths are reflected by the material leading to its coloration. Besides the aesthetical function, the color of the fabric is one of the most important variables on the protection against UV radiation [10]. There are several characteristics, such as chemical structures of the dyestuff and the shade and intensity of the color that may influence the improvement of UV protection. Dark colors have been reported as providing better protection than light colors [4, 6, 11, 12]. UV radiation with  $300 \leq \lambda \leq 400$  nm, representing up to 5 % of the total incident sunlight on the earth surface, has the highest quantum energy [1, 13]. This energy may affect the structure of fabric substrate, the structure of dye molecules, and the chemical bonding between the dye and the fabric support. The reactive azo-triazine dyes are among the most common classes of substances used for coloring textiles. During the dyeing process, the reactive dyes are covalently bonded to the textile [14]. The chemical structures of these dyes contain one or more azo bonds (R-N = N-R) that provide visible light absorption [12]. A wide range of chromophores with excellent fastness can be selected including various triazine derivatives [14]. Unlike direct dyes, which create weak hydrogen bonding with the cellulose substrate, the reactive dyes can also be attached to the fiber by covalent bonding between the reactive dye group, such is a halo-heterocycle (i.e. halo-triazine) or an activated double bond, and nucleophilic fiber group, thus exhibiting a greater light stability and fast washing characteristics [15, 16]. Halo-triazine structures are among

L. Rosu · D. Rosu (✉) · C.-D. Varganici  
Centre of Advanced Research in Bionanoconjugates and Biopolymers, “Petru Poni” Institute of Macromolecular Chemistry, 41A Gr. Ghica-Voda Alley, 700487 Iasi, Romania  
e-mail: drosu@icmpp.ro; dan\_rosu50@yahoo.com

C.-C. Gavat  
University of Medicine and Pharmacy “Gr T Popa” Iasi,  
16 University Street, 700115 Iasi, Romania

the most common reactive groups able to react with  $-OH$  or  $-NH_2$  groups belonging to cellulose or proteic fibers. Therefore, dyeing with reactive dyes has become the most common method for coloring of some cellulosic textile materials such as cotton [14]. Because of its simplicity, the method is successfully used both in industry and at home or in the art studio. Usually, the colored fabrics remain in contact with the human skin for several hours every day [17]. It is known that the azo dyes can undergo some biochemical changes leading to colorless compounds with aromatic amine structure, which are easily absorbed by the skin [17]. An important role in the chemical transformations of dyes molecules which come in contact with the skin surface is played by bacteria. Although some of the metabolites show low toxicity compared with the original compounds [18], some papers report that the aryl amines structures and the free radicals are potentially carcinogenic [19–21]. It is also known that the dye base triazines are the major sources of pollution to the environment. The preliminary pathological studies on rats have shown that some reactive dyes with azo-triazine structures have a high toxic potential (Reactive Yellow-143 and Reactive Orange-13) while others presented moderately toxic characteristics (Reactive Red-2 and Reactive Red-183) [22]. Although studies on the photostability of reactive dyes in solution were reported in the literature [14, 23, 24], the influence of UV radiation on textiles painted with azo-triazine dyes is less known. Since the stability of the fabric-dye complex may affect human health, the aim of this paper consists in the assessment of the photodecomposition behavior of the dyed textile under the action of UV radiation with  $\lambda > 300$  nm.

## Materials and methods

### Materials

Four reactive dyes with azo-triazine structures were received and previously purified by recrystallization from methanol: Reactive Yellow 143 (RY-143), Reactive Orange 13 (RO-13), Reactive Red 183 (RR-183), and Reactive Red 2 (RR-2). Some additional data such as chemical structures, provider companies, UV absorption peaks ( $\lambda_{max}$ ), and the molecular weights ( $M_w$ ) that characterize the reactive dyes used in the study are presented in Table 1.

According to the literature data, the peaks with the maximum absorption signals values of  $\sim 280$  and  $\sim 230$  nm correspond to triazine and to benzene entities [25]. Also, the signals ranging between 400 and 600 nm are specific to the conjugated electronic system which characterizes the chromophores. The cleavage of the chromophoric entities under

UV irradiation leads to the decoloration of the dyes structures [25] and of the dyed fabrics, as a consequence. The accumulation of chromophores resulted from photo-oxidation processes of dye and/or textile support leads to darkening of irradiated samples. A fabric, manufactured mainly of alkaline cleaned and bleached cotton fibers, was obtained from a commercial source (IASITEX S.A. Iasi, Romania). Fabric dyeing was achieved by fleet depletion technique in alkaline media (pH 9–10) with computerized plant Mathias Polycolor Uniprogramer 2002 type (Werner Mathias AG, Switzerland). Aqueous solutions containing 5 % dye were used to paint the fabric. The temperature in the dyeing bath increased from 21 to 80 °C with a heating rate of 5 °C  $min^{-1}$ . Rinsing with hot water, cold water, and finally, with distilled water was used to remove the traces of unreacted dye.

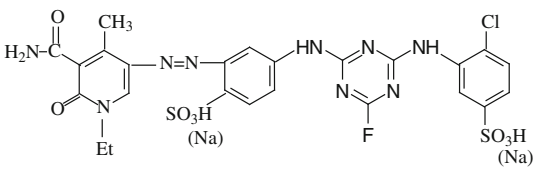
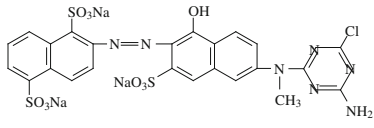
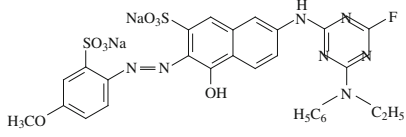
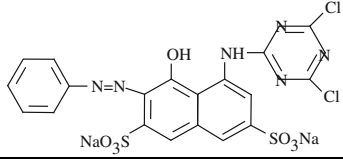
### Irradiation

49-cm<sup>2</sup>-dyed fabric was irradiated with a medium pressure OSRAM HQE-40 lamp, as an artificial light source, in the field range of 240–400 nm. The light source power was 100 W. Irradiation of fabric samples was performed in air by using a rotating hexagonal prism shaped device, as sample carrier, with the light source positioned on the central axis of the prism. Samples were protected from thermal degradation with a distilled water filter and a fan. The more energetic radiations with  $\lambda < 300$  nm, not present in the natural light spectrum, were eliminated with a quartz/borosilicate filter having a maximum transparency at 365 nm. The irradiance value, measured at a distance of 60 mm from the source, was 9.7 mW  $cm^{-2}$ . This value was about 4.4 times higher than the average UV irradiance measured outdoors on a clear summer day (2.2 mW  $cm^{-2}$ ). A PMA 2100 radiometer provided with a UVA detector, type PMA 2110 (Solar Light Co., USA) was used for measurements of irradiance and of radiance exposure which is dependent on the irradiation time. The temperature measured inside of the irradiation device was 20–22 °C and the relative air humidity (RH) was 53 %. A thermo-hygrometer model JK-HTM-3 (Shanghai Jingke Scientific Instrument Co., China) was used to monitor the temperature and RH values during irradiation. Samples were extracted from the irradiation device every 20 h and analyzed.

### Analytical methods

The color analysis was performed with a PocketSpec apparatus purchased from Color QA SUA with a sensor head of 6 mm. A super white sulfate barium pellet was used to calibrate the device. Measurements were conducted in reflectance mode using D<sub>65</sub> illuminant at 10° standard

**Table 1** The characteristics of the reactive azo-triazine dyes

Name/Manufacturer	Chemical formula	$\lambda_{\max}$	$M_w$
Reactive Yellow 143 (RY-143)/ Hutsman Textile effects		217, 265, 422	742.02
Reactive Orange 13 (RO-13)/ Hutsman Textile effects		226, 284, 488	762.03
Reactive Red 183 (RR-183)/ Hutsman Textile effects		227, 280, 503	713.62
Reactive Red 2 (RR-2)/ PRO Chemical & Dye		217, 289, 544	615.33

observer. The results were presented in the CIELAB system. The color changes were evaluated by monitoring the variation of the lightness factor ( $L^*$ ) and of chromatic coordinates: redness-greening ( $a^*$ ) and yellowness-blueness ( $b^*$ ) before and after irradiation. The color variation caused by irradiation ( $\Delta E_{ab}$ ) was calculated using Eq. (1), proposed by the International Commission on Illumination (CIE) in 1976:

$$\Delta E_{ab} = \sqrt{(L_2^* - L_1^*)^2 + (a_2^* - a_1^*)^2 + (b_2^* - b_1^*)^2}, \quad (1)$$

where 1 and 2 indexes correspond to the parameters recorded before and after irradiation.

Samples were analyzed for color changes according to DIN 6174 (Farbmetrische Bestimmung von Farbständen bei Körperfarben nach der CIELAB-Formel, 1979).

The UV–Vis spectra and quantitative determination of the dyes detached from the cellulosic fibers, as a result of exposure of fabrics to UV radiation, were made with UV–

Vis Cole Palmer 1100 RS apparatus provided with Unico 1100 SS-1.11 version software. Measurements were carried at the visible wavelengths corresponding to the absorption peaks that characterize each dye. Concentrations of extracted dyes were calculated using the standard previously plotted curves. The dyes extraction solutions were prepared according to the standard SR EN ISO 105-E04, January 1998, classification index L22, Textiles—Tests for color fastness to perspiration, using the prescriptions given below [26].

For the alkaline extraction, a freshly prepared solution containing 0.1 g  $\alpha$ -L alanine, 1 g NaCl, and 0.5 g  $\text{Na}_2\text{HPO}_4 \cdot 2\text{H}_2\text{O}$  was used. The solid substances were dissolved in 200 mL distilled water and the pH values were adjusted to 8 using a 0.1 mol  $\text{L}^{-1}$  NaOH solution. For the acid extraction, a freshly prepared solution containing 0.1 g  $\alpha$ -L alanine, 1 g NaCl, and 0.5 g  $\text{NaH}_2\text{PO}_4 \cdot 2\text{H}_2\text{O}$  was used. The solid substances were dissolved in 200 mL distilled water and the pH values were adjusted to 5.5 using a

0.1 mol L<sup>-1</sup> NaOH solution. The pH value was monitored with an AB 15 Plus Cole Parmer device provided with a glass electrode Accumet BASIC.

Near infrared chemical imaging (NIR-CI) spectra were recorded on a Specim's Ltd. SisuCHEMA device controlled with Evince software package for processing the original image data. The system includes a chemical imaging workstation for 1000–2500 nm, NIR 130 domains. The original image for each sample was taken with a NIR model spectral camera, respectively an imaging spectrograph type ImSpector N17E with 320 and 640 pixel spatial resolution at a rate of 60–350 Hz.

## Results and discussion

### Color changes during irradiation and photodecomposition mechanism

The color changes as function of irradiation dose for the fabrics painted with reactive dyes in Table 1 are presented in Fig. 1.

Color differences significantly increased with the irradiation dose for all the studied samples. The samples painted with light colored dyes, such as RY-143 and RO-13, presented the highest damage caused by irradiation. It is possible in these cases that the dyes layers may be easily penetrated by the UV radiations thereby causing a more advanced photochemical degradation of the cellulosic fabric. The fabrics painted with dyes RR-183 and RR-2 were less sensitive to irradiation. In this case, the color differences recorded during irradiation were comparable

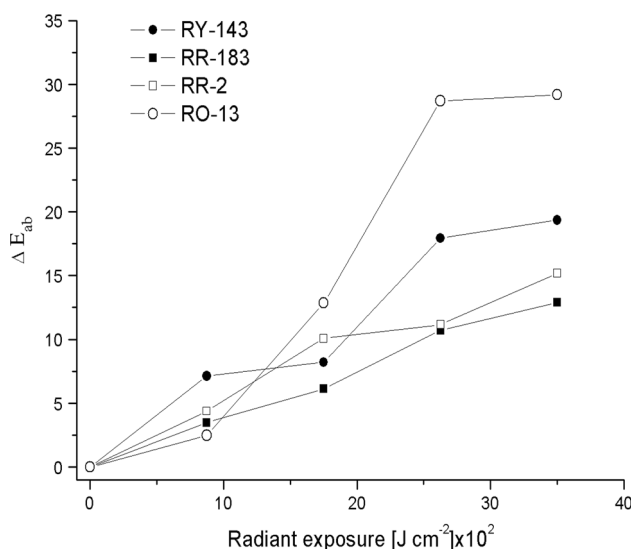


**Fig. 1** The color changes of the studied samples as a function of irradiation dose

and significantly lower than those recorded for the samples painted with RY-143 and RO-13.

The lightness factor variation ( $L^*$ ) with irradiation dose is depicted in Fig. 2.

A high darkening tendency of fabrics painted with RY-143 and RO-13 during irradiation was found, while an insignificant modification of  $L^*$  values of the fabrics painted with RR-2 and RR-183 was observed. The variation of  $a^*$  and  $b^*$  after exposure to different irradiation doses is shown in Table 2.

The increase of irradiation doses caused the decrease of chromatic coefficients values in the case of fabrics painted with all studied dyes. The samples behaved as if they accumulated blue and green chromophores during irradiation. It is possible for the structural changes of dye molecules during irradiation to lead to a simultaneous hypochrome and bathochrome displacement of the absorption maxima, thus coloring the sample in complementary colors (blue and green). Changes in visible absorption spectra as a result of irradiation support these observations, as can be observed in Fig. 3.

Figure 3 shows the decrease of maximum absorption intensities for all the studied dyes during irradiation, as if the samples suffer loss of dye during irradiation. Broadening of the absorption spectra toward higher wavelengths, up to 800 nm, during irradiation was also observed. This behavior supports the idea of new chromophores accumulation on the surfaces of the irradiated samples. The photodecomposition mechanism of the textile painted with the azo dyes was of high complexity. It is known from the literature that darkening of azo dyes is the result of complex photo-oxidation phenomena due to C–N bond

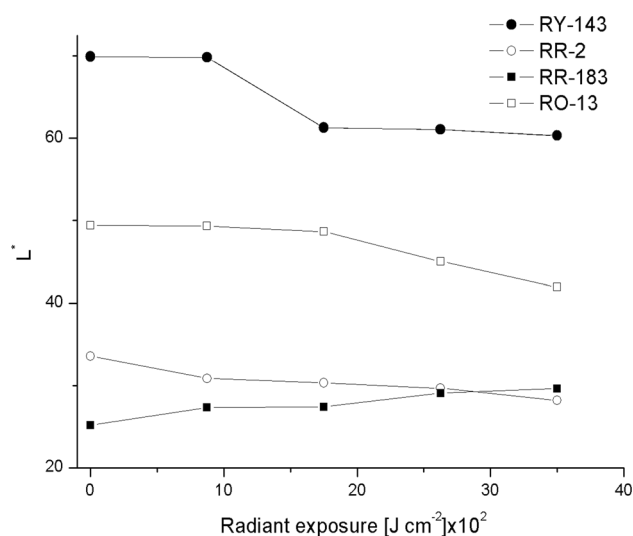


**Fig. 2** The lightness factor variation ( $L^*$ ) with irradiation dose as a function of irradiation dose

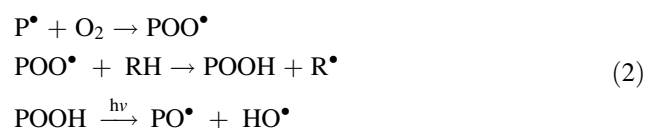
**Table 2** Variation of chromatic coefficients with radiation dose

Fabric type	Radiant exposure (J cm <sup>-2</sup> × 10 <sup>2</sup> )	a*	b*
RY-143	0	-12.57	64.79
	8.75	-10.99	63.25
	17.5	-9.25	56.12
	26.25	-7.91	50.38
	35.0	-6.99	49.68
	0	33.83	40.82
RO-13	8.75	22.98	29.23
	17.5	21.29	26.92
	26.25	17.09	22.86
	35	15.35	21.43
	0	48.52	36.36
RR-183	8.75	44.19	32.97
	17.5	41.97	30.98
	26.25	40.55	29.30
	35.0	39.04	27.62
	0	48.26	24.03
RR-2	8.75	46.42	20.09
	17.5	42.10	17.05
	26.25	42.54	14.62
	35.0	39.25	11.90

cleavage from the amine moieties (Scheme 1), leading to the formation of blue chromophores [27]. As an exemplification, Scheme 2 shows the formation of blue chromophores from radical IX, resulted during photodecomposition of RY-143, due to the other dyed textiles similar photochemical behavior. Physically absorbed water may generate H<sup>+</sup>, thus assuring an acid media and oxygen from air.

As an observation, the significant decrease in *L\** values may be correlated with the substitution degree and number of amine moieties, which is higher for the fabrics painted with RY-143 and RO-13 compared to RR-2 and RR-183, thus leading to bathochrome displacement effect and blue and green chromophore accumulation. The hypochrome effect may be also due to photochemical cleavage of azo bond [28].

The photo-degradation process may be initialized by a series of free radicals, HO•, generated via hydroperoxide decomposition, where *R* and *P* may be impurities, additives, or other organic radicals [28]. As an exemplification, Eq. (2) shows the formation of hydroxyl radicals via photochemical decomposition of hydroperoxydes.



As an exemplification, Scheme 3 depicts a general photodecomposition mechanism of textile dyed with RY-143. Primary intermediates generate an irreversible attack on the chromophoric moieties of the dye molecule, leading to their destruction and N<sub>2</sub> evolution. The radical attack occurs both on the azo group and directly on the aromatic rings [28]. This aspect leads to the occurring of the hypochromic effect, which consists of a decrease in absorption spectra intensity, due to the photodecomposition of azo bond disturbing the conjugation [29].

The modifications of UV-Vis spectra may explain the changes in color parameters of the dyed textile fabric during irradiation. Even the cellulosic fabric could undergo some photo-oxidative degradation during exposure to UV radiation, the dye acting as a photo-sensitizer. It is known that the UV radiation may cause the generation of free radicals that are able to initiate photo-degradative reactions in the cellulosic materials such as depolymerization, dehydrogenation, dehydroxylation, dehydroxymethylation, and the release of hydrogen, carbon monoxide, and carbon dioxide [30]. Photo-oxidative reactions are involved mainly in cellulose depolymerization [30]. The appearance of new chromofore groups with conjugated unsaturated structures as a result of photo-oxidation processes in the cellulose fibers can also explain the color changes of colored textiles [31].

There are no differences between the FTIR spectra of the studied samples recorded at wavenumber values between 4000 and 400 cm<sup>-1</sup> and that of the textile substrate. Figure 4 shows, as an example, the FTIR spectrum of the cellulosic fabric dyed with RY-143, recorded before irradiation, the other samples showing identical FTIR spectra.

The broad band between 3600 and 3000 cm<sup>-1</sup> is attributed to the cellulosic OH groups stretching vibration. The peak at 2901 cm<sup>-1</sup> corresponds to C–H stretching vibrations. The peak at 1428 cm<sup>-1</sup> is assigned to a symmetric CH<sub>2</sub> bending vibration. According to the literature [32], this band may give information on the crystallinity of the cellulosic substrate. The peak at 1645 cm<sup>-1</sup> is assigned to absorbed OH or conjugated C=O entities. The peak at 1365 cm<sup>-1</sup> is attributed to symmetric C–H deformation, the peak at 1316 cm<sup>-1</sup> to CH<sub>2</sub> wagging, the one at 1203 cm<sup>-1</sup> to OH deformation and the peak at 1158 cm<sup>-1</sup> to C–O–C asymmetric vibration. The region from 1107 to 900 cm<sup>-1</sup> corresponds to asymmetric glucose ring and C–O stretching vibrations [33]. The peak at 900 cm<sup>-1</sup> is related to β-(1 → 4)-glycosidic bonds stretching vibration. This band may provide information on the amorphous state of the cellulosic substrate [32].

Two absorption regions exhibited significant modification after irradiation : the range specific to to glucose ring

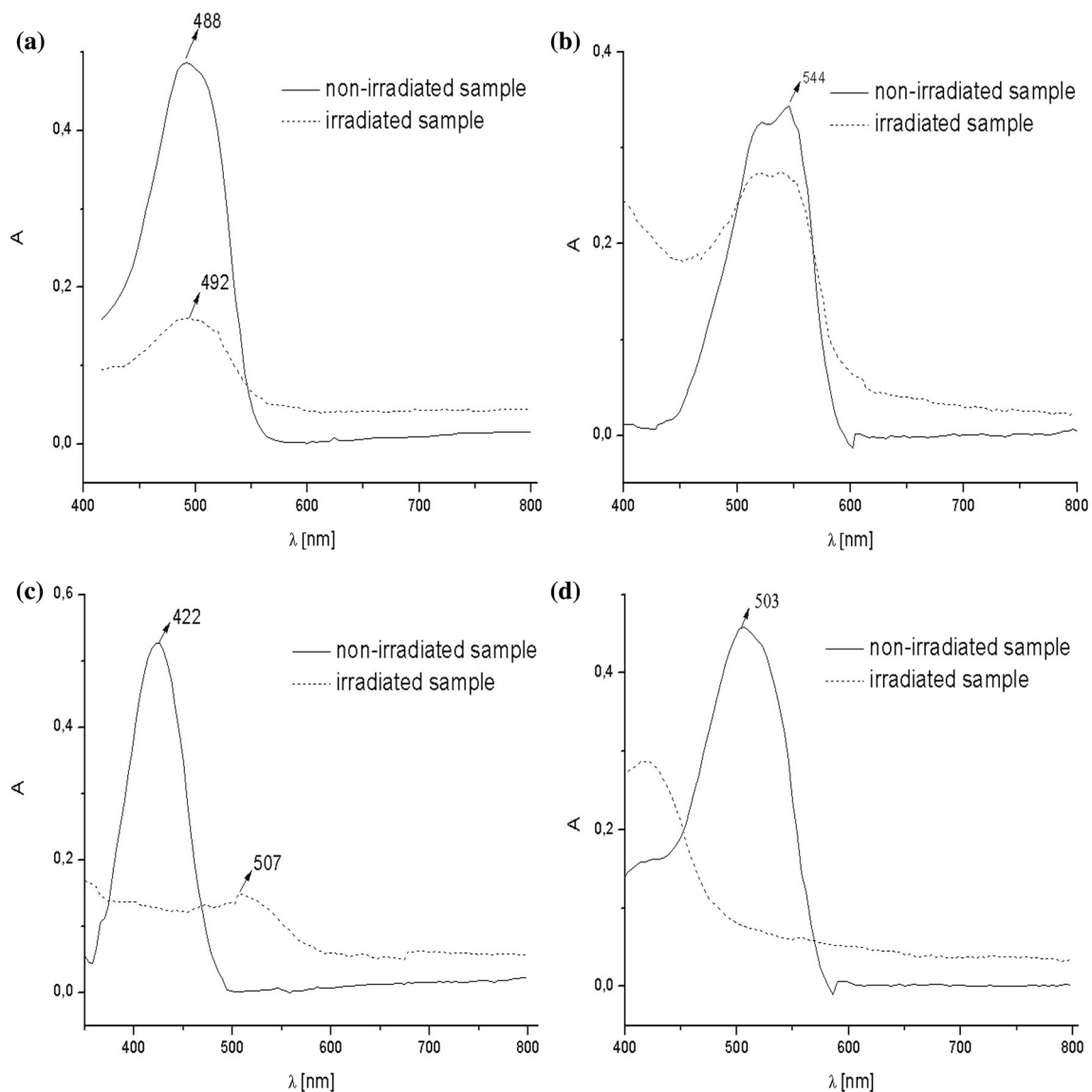


**Fig. 3** Changes in visible absorption spectra as a result of irradiation for: **a** RO-13; **b** RR-2; **c** Y-143; **d** RR-183

(1200–800  $\text{cm}^{-1}$ ) (Fig. 5) and carbonyl groups (1800–1550  $\text{cm}^{-1}$ ) (Fig. 6).

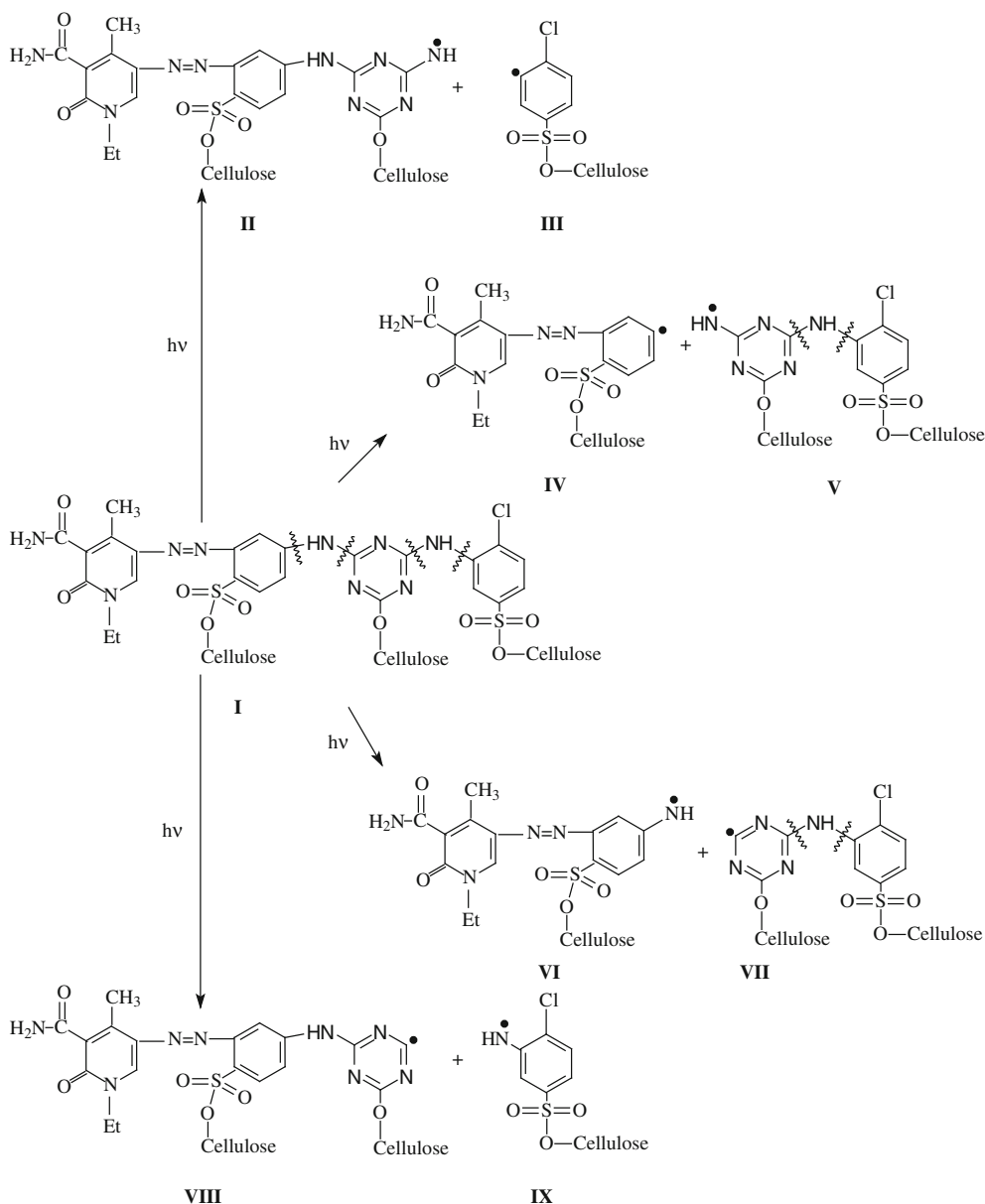
The appearance of new signals at 1728, 1649, and 1641  $\text{cm}^{-1}$  is a sign of photo-oxidation phenomena occurrence on the surface of the cellulosic substrate, while the increase of peak signals in the glucose ring absorbance domain indicates a lowering of the molecular mass of glucose chains, most probably from chain ends with liberation of glucose units. Dye molecules which are covalently bonded by glucose units may be dissolved by perspiration, therefore causing adverse effects to human skin. The amount of dye separated from the fabric depends on the irradiation dose. Figure 7 presents the variation of amount of dye extracted with low acidic and basic

solutions and distilled water as a function of irradiation exposure dose.

Two observations can be made regarding Fig. 7. Firstly, an increase in the extracted dye quantity with irradiation dose can be observed. This aspect can be related to a more intense photo-degradation of the cellulose substrate. Secondly, higher values of the pH lead to the extraction of higher dyes quantities from the cellulose textiles.

#### Structural modifications studies by NIR-CI spectroscopy

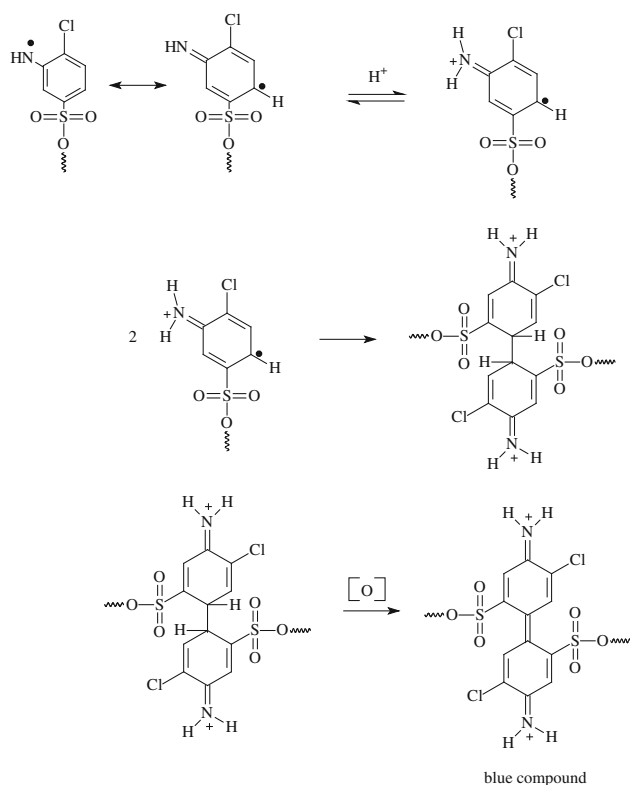
Samples of non dyed textile fabric, dyed textile fabrics, and dyed and UV irradiated textile fabrics for 100 h at an



**Scheme 1** Cleavage of C–N bonds during photodegradation of fabric painted with RY-143

irradiation dose of  $3500 \text{ J cm}^{-2}$  were characterized by means of NIR-CI technique. NIR-CI is a simple and relatively rapid quantitative analytical method which requires no special sample preparation. Only the equipment calibrations are time consuming. This method provides information on the spatial distribution of the comprising components of a sample, provided by a chemical image [34–36]. This aspect also enables the evaluation of the degree of the physical and/or chemical heterogeneity for a given sample [37–39]. The chemical images are visualized as three-dimensional data blocks and are used for the partial least squares-dynamic analysis (PLS-DA) by means of Evince software. Through PLS-DA method, the obtained

spectral data is decomposed into a set of small number of classification scores. These scores are obtained based on the correlation of the information from both the spectral and response variables. The NIR-CI technique was also implied to monitor the chemical structures. This aspect is possible because this method can show the changes of different functional groups at the dye-textile interface [40–42]. Figure 8 corresponds to the PLS-DA model for non dyed textile fabric, dyed textile fabrics, and dyed and UV irradiated textile fabrics for 100 h. Figure 8 shows that gray is the predominant color in the most regions of the score. This aspect indicates that the dye is well dispersed within the textile surface. An increase in the color



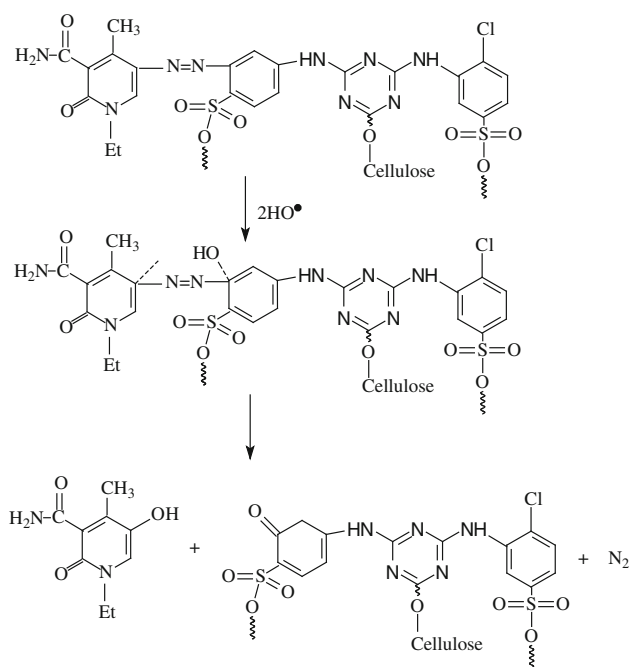
**Scheme 2** Formation of blue chromophores during photoirradiation of RY-13

amplitude during irradiation can also be observed, suggesting structural modifications within the dyed textile fabric.

The experimental signal values for each functional group were assigned by using IR reference spectra within the NIST spectral library database.

The following NIR-CI absorption bands values were assigned to the dyed textile fabric: Y-143: wide band 1470–1735 nm (N–H stretch first overtone); wide band 1960 nm (O–H stretch/O–H bend combination); 2135 nm (C–H stretch/C=O stretch combination or symmetric C–H deformation); RO-13: 1645 nm (C–H first overtone); 1973 nm (N–H asymmetric stretch/N–H in plane bend/C–N stretch combinations); 2104 nm (O–H bend combination) (Fig. 9); RR-183: 1470 nm (N–H stretch first overtone); 1975 nm (N–H asymmetric stretch/N–H in plane bend/C–N stretch combinations); 2095 nm (C–H combination); 2280 nm (C–H stretch/CH<sub>2</sub> deformation); RR-2: 1780 nm (C–H stretch); 2375 nm (C–H stretch/C–C stretch combination).

NIR absorption bands assigned to the dyed and UV irradiated textile fabrics for 100 h: Y-143: 985 nm (N–H second overtone); 2135 nm (O–H stretch/C=O stretch combination/symmetric C–H deformation); 2280 nm (C–H stretch/CH<sub>2</sub> deformation); RO-13: 1540 nm (O–H stretch first overtone); 2110 nm (O–H bend/C–O stretch



**Scheme 3** Photooxidative decomposition mechanism of chromophore structures of RY-13

combination and asymmetric C–O–O stretch third overtone from the new peroxide structures probably formed during irradiation); 2295 nm (C–H bend second overtone) 2450 nm (C–H combination and symmetric C–N–C stretch overtone); RR-183: 1790 nm (O–H combination); 1980 nm (asymmetric N–H stretch/N–H in-plane bend C–N stretch combination); 2100 nm (asym C–O–O stretch third overtone from new peroxide structures formed during irradiation); RR-2: 1505 nm (N–H stretch first overtone); 1705 nm (C–H stretch first overtone).

## Conclusions

Structural and color modifications of textile materials painted with four different azo-triazine dyes were studied during 100 h UV irradiation time and an irradiation dose up to 3500 J cm<sup>-2</sup>. Structural changes during irradiation were compared by applying FTIR, UV–Vis, and NIR-CI techniques. A darkening tendency of fabrics painted with RY-143 and RO-13 during irradiation was found, while an insignificant modification of the *L*\* values of the fabrics painted with RR-2 and RR-183 was observed. This aspect was explained by the accumulation of blue and green chromophores during irradiation, due to photo-oxidation reactions on the cellulose substrate surface. Changes in visible absorption spectra as a result of irradiation supported these observations. A photodecomposition mechanism of dyes was proposed. It was concluded that the UV



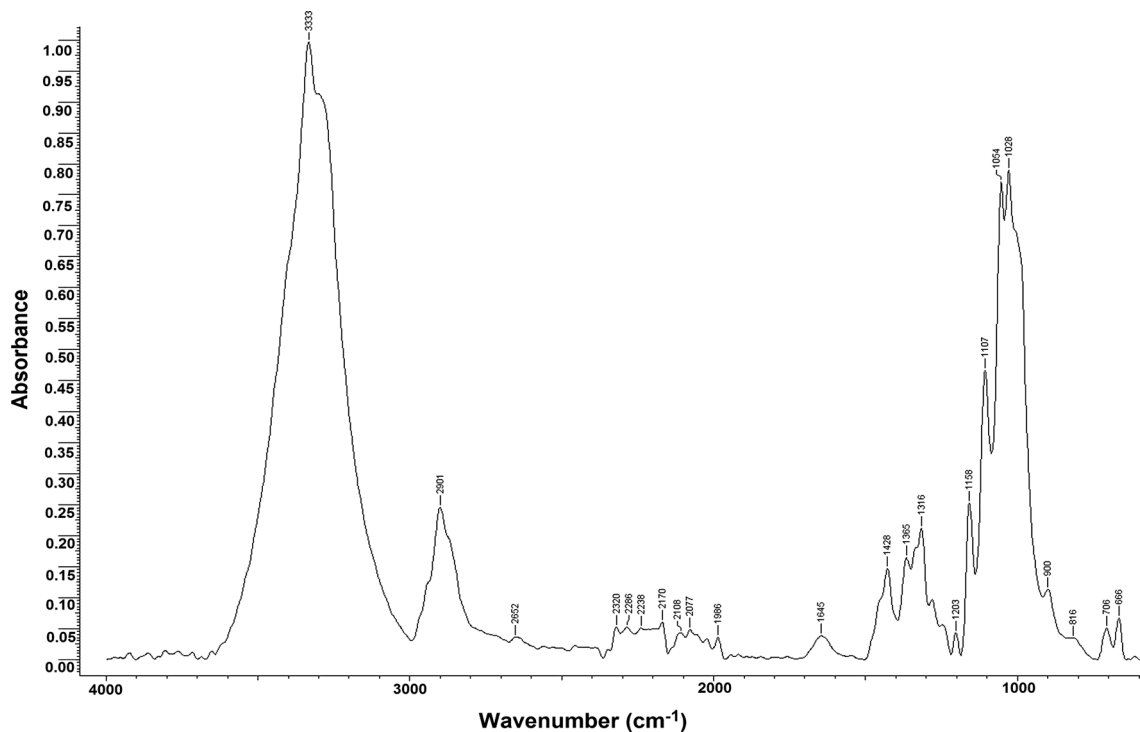


Fig. 4 FTIR spectrum of the cellulosic fabric dyed with RY-143

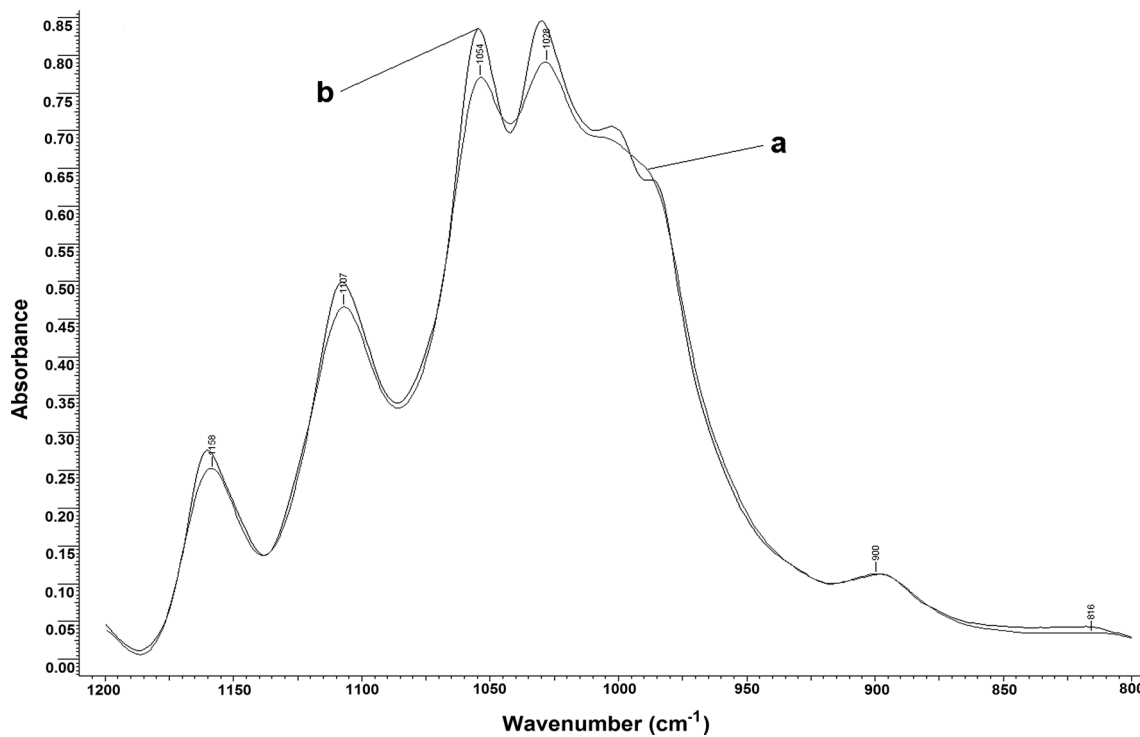
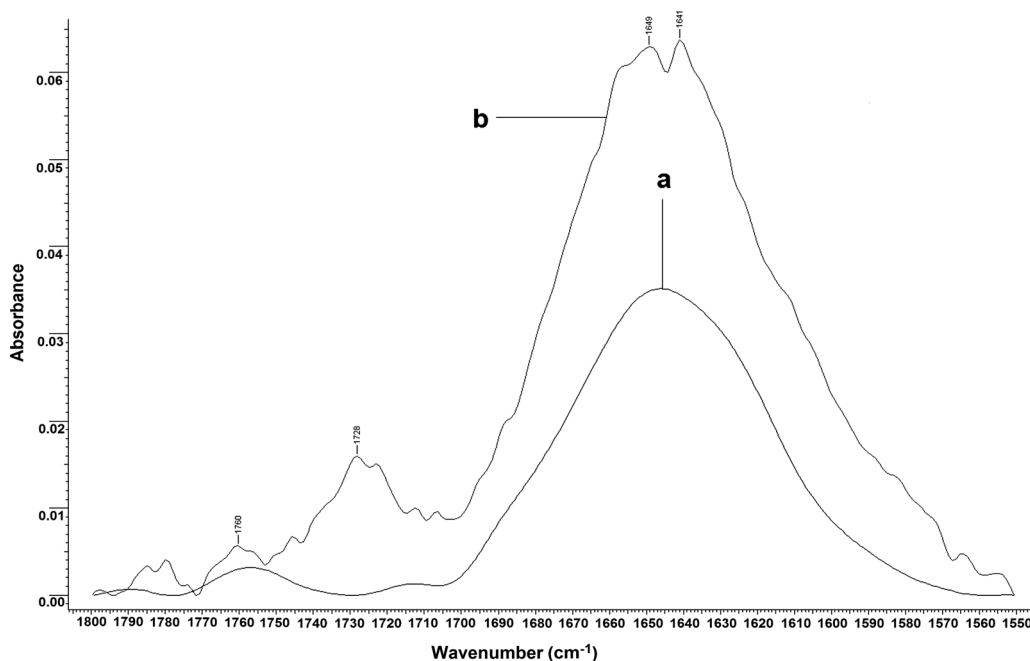
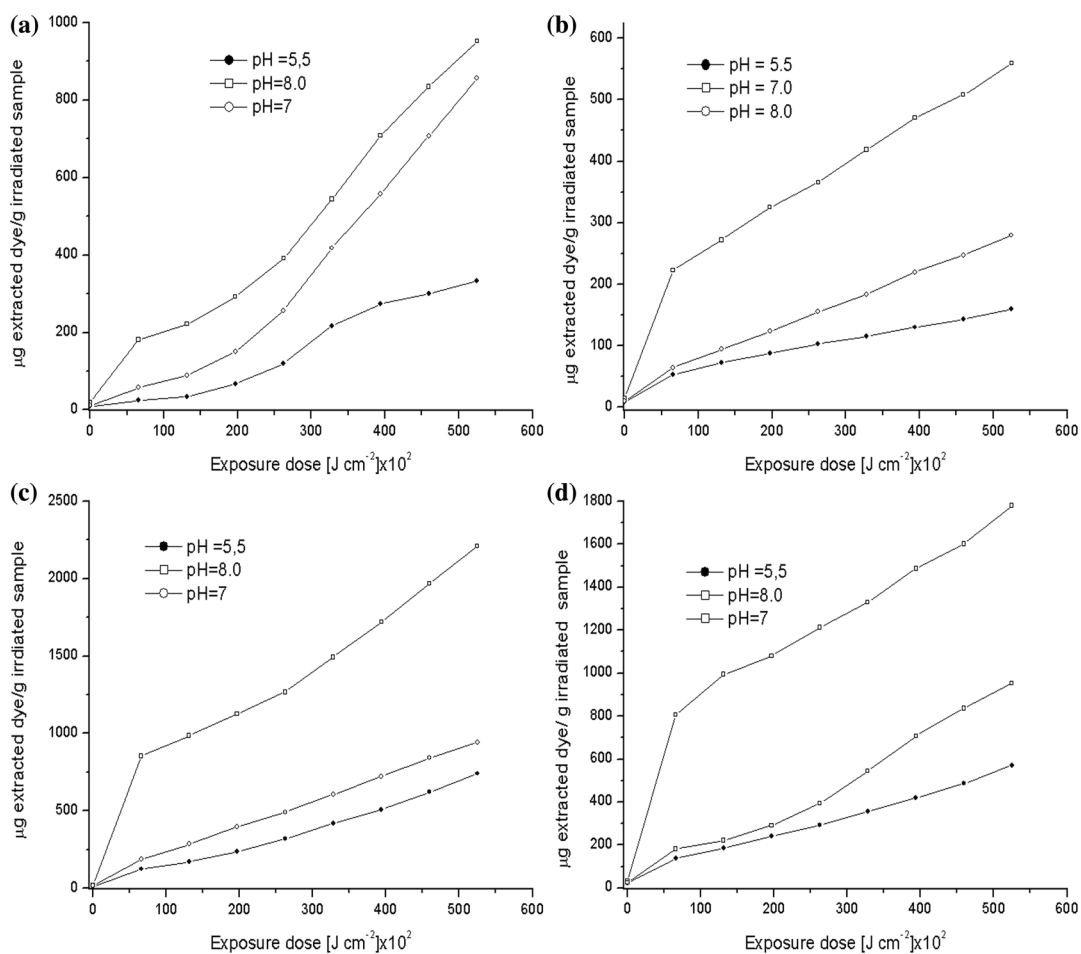


Fig. 5 Comparative FTIR spectra of RY-143 dyed textile fabric the range specific to glucose ring: *a* before and *b* after irradiation



**Fig. 6** Comparative FTIR spectra of RY-143 dyed textile fabric the range specific to carbonyl groups: *a* before and *b* after irradiation



**Fig. 7** Quantity of extracted dye per gram irradiated sample as a function of irradiation dose and pH of extraction solutions: (a) RY-143; (b) RR-183; (c) RR-2; (d) RO-13

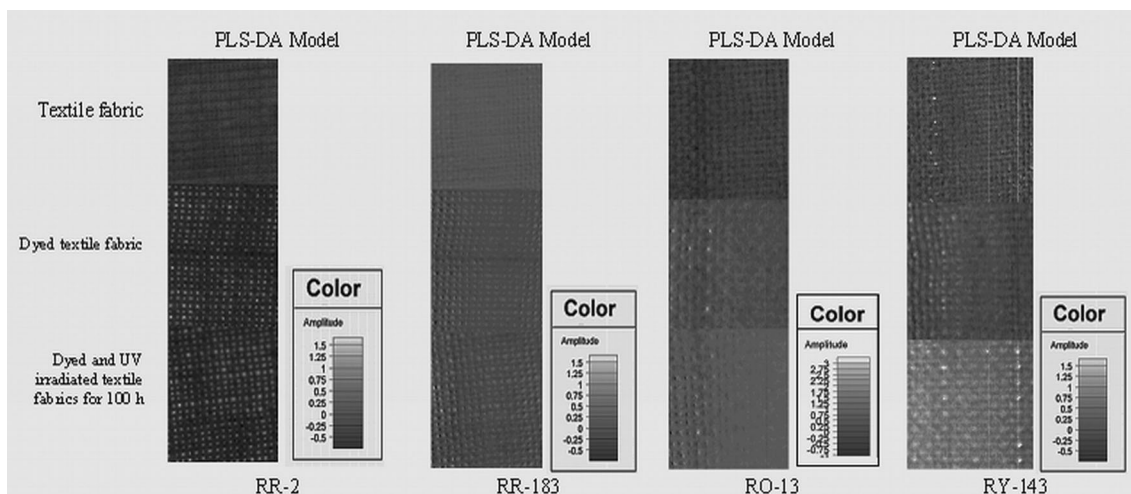


**Fig. 8** PLS-DA model for non dyed textile fabric, dyed textile fabrics and dyed and UV irradiated textile fabrics for 100 h

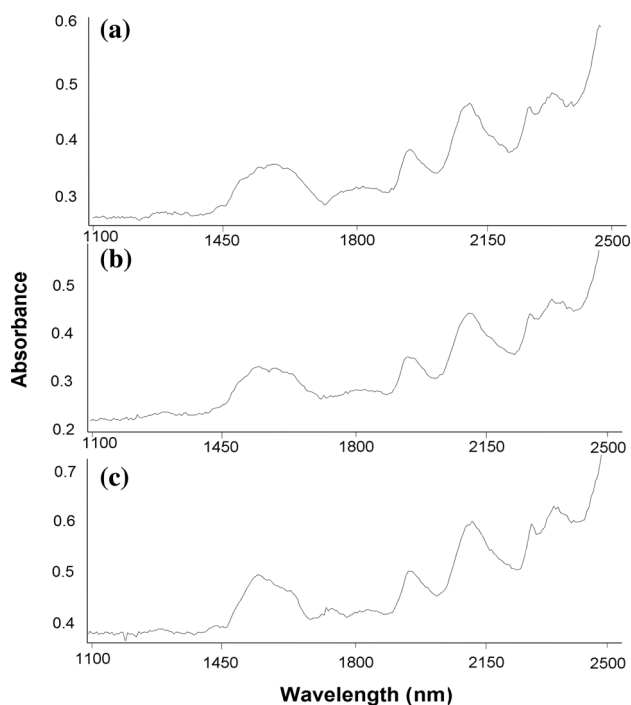


**Fig. 9** NIR-CI reflectance spectra of RO-13: **a** non-dyed textile fabric; **b** dyed textile fabric and **c** dyed and UV irradiated textile fabric for 100 h

exposure led to the partial detachment of the dyes from the textile surfaces, together with glucose units and dye photodegradation by C–N bond cleavage and destruction of azo chromophore groups and aromatic rings. NIR spectra showed possible peroxidation processes in the structures of the fabrics dyed with RO-13 and RR-183.

**Acknowledgements** Authors acknowledge the financial support of a grant of the Romanian National Authority for Scientific Research,

CNCS—UEFISCDI, Project Number PN-II-ID-PCE-2011-3-0187. Authors are grateful to Ph.D. student Manuela-Tatiana Nistor of the “Petru Poni” Institute of Macromolecular Chemistry, Iasi, Romania, for the recording of the NIR spectra. Paper dedicated to the 65th anniversary of “Petru Poni” Institute of Macromolecular Chemistry of Romanian Academy, Iasi, Romania.

## References

1. Biswa RD (2010) UV radiation protective clothing. *Open Text J* 3:14–21
2. Riva A, Agaba I, Pepio M (2006) Action of a finishing product in the improvement of the ultraviolet protection provided by cotton fabrics. *Model Eff Cell* 13(6):697–704
3. Hilfiker R, Kaufmann W, Reinert G, Schmidt E (1996) Improving sun protection factors of fabrics by applying UV-absorbers. *Text Res J* 66(2):61–70
4. Algaba I, Pepio M, Riva A (2007) Modelisation of the influence of the treatment with two optical brighteners in the UPF of cellulosic fabrics. *Ind Eng Chem Res* 46(9):2677–2682
5. Grifoni D, Bacci L, Zipoli G, Albanese L, Sabatini F (2011) The role of natural dyes in the UV protection of fabrics made of vegetable fibres. *Dyes Pigments* 91:279–285
6. Srinivasan M, Gatewood B (2000) Relationship of the dye characteristics to UV protection provided by cotton fabric. *Text Chem Color Am D* 32(4):36–43
7. Crews P, Kachman S, Beyer A (1999) Influences of UVR transmission of dyed woven fabrics. *Text Chem Color* 31(6):17–26
8. Reinert G, Fuso F, Hilfiker R, Schmidt E (1997) UV protecting properties of textile fabrics and their improvement. *AATCC Rev* 29(12):31–43
9. Muruganandham M, Swaminathan S (2007) Solar driven decolourisation of Reactive Yellow 14 by advanced oxidation processes in heterogeneous and homogeneous media. *Dyes Pigments* 72(2):137–143
10. Dubrovski PD, Golob D (2009) Effects of woven fabric, construction and color on ultraviolet protection. *Text Res J* 79(4):351–359
11. Gorenssek M, Sluga F (2004) Modifying the UV blocking effect of polyester fabric. *Text Res J* 74(6):469–474

12. Stingley RL, Zou W, Heinze TM, Chen H, Cerniglia CE (2010) Metabolism of azo dyes by human skin microbiota. *J Med Microbiol* 59:108–114
13. Rosu D, Rosu L, Mustata F, Varganici CD (2012) Effect of UV radiation on some semiinterpenetrating polymer networks based on polyurethane and epoxy resin. *Polym Degrad Stab* 97:1261–1269
14. Kusic H, Koprivanac N, Bozic AL (2013) Environmental aspects on the photodegradation of reactive triazine dyes in aqueous media. *J Photochem Photobiol A* 252:131–144
15. Alinsafi A, da Motta M, Le Bonte A, Pons MN, Benhammou A (2006) Effect of variability on the treatment of textile dyeing wastewater by activated sludge. *Dyes Pigments* 69:31–39
16. Laing IG (1991) The impact of effluent regulations on the dyeing industry. *Rev Prog Color* 21:56–71
17. Golka K, Kopps S, Mislak ZW (2004) Carcinogenicity of azo colorants: influence of solubility and bioavailability. *Toxicol Lett* 151:203–210
18. Collier SW, Storm JE, Bronaugh RL (1993) Reduction of azo dyes during in vitro percutaneous absorption. *Toxicol Appl Pharm* 118:73–79
19. Nakayama T, Kimura T, Kodama M, Nagata C (1983) Generation of peroxide and superoxide anion from active metabolites of naphthylamines and aminoazo dyes: its possible role in carcinogenesis. *Carcinogenesis* 4:765–769
20. Chung KT (1993) The significance of azo-reduction in the mutagenesis and carcinogenesis of azo dyes. *Mutat Res* 114:269–281
21. Mason RP, Peterson FJ, Holtzman JL (1977) The formation of an azo anion free radical metabolite during the microsomal azo reduction of sulfonazo III. *Biochem Biophys Res Commun* 75:532–540
22. Gavatt CC (2011) Contributions to knowledge involvement of reactive dyes in determining the biological effects, in conjunction with their physical and chemical properties. Ph.D. Thesis, “Gr.T.Popa” University, Faculty of Pharmacy, Iasi
23. Chatterjee D, Rupini Patnam V, Sikdar A, Joshi P, Misra R, Rao NN (2008) Kinetics of the decoloration of reactive dyes over visible light-irradiated TiO<sub>2</sub> semiconductor photocatalyst. *J Hazard Mater* 156:435–441
24. Khataee AR, Pons MN, Zahraa O (2009) Photocatalytic degradation of three azo dyes using immobilized TiO<sub>2</sub> nanoparticles on glass plates activated by UV light irradiation: influence of dye molecular structure. *J Hazard Mater* 168:451–457
25. Cocca M, Arienzo LD, Orazio LD (2011) Effects of different artificial agings on structure and properties of Whatman paper samples. *ISRN Mat Sci*. doi:10.5402/2011/863083
26. Marques MRC, Loebenberg R, Almukainzi M (2011) Simulated biological fluids with possible application in dissolution testing. *Dissolut Technol* 8:15–28
27. McKellar JF (1965) The photo-oxidation of an aromatic amine studied by flash photolysis. *Proc R Soc Lond A* 287:363–380
28. Wojnárovits L, Takács E (2008) Irradiation treatment of azo dye containing wastewater: an overview. *Rad Phys Chem* 77:225–244
29. Burdzinski G, Kubicki J, Maciejewski A, Steer RP, Velate S, Yeow EKL (2006) Photochemistry and photophysics of highly excited valence states of polyatomic molecules: nonalternant aromatics, thioketones and metalloporphyrins. In: Ramamurthy V, Schanze KS (eds) *Organic photochemistry and photophysics*. CRC Press, Boca Raton, p 17
30. Kavler K, Gunde-Cimerman N, Zalar P, Demšar A (2011) FTIR spectroscopy of biodegraded historical textiles. *Polym Degrad Stab* 96:574–580
31. Yatagai M, Zeronian SH (1994) Effect of ultraviolet light and heat on the properties of cotton cellulose. *Cellulose* 1:205–214
32. Ciolacu D, Ciolacu F, Popa VI (2011) Amorphous cellulose structure and characterization. *Cell Chem Technol* 45:13–21
33. Pandey KK (1999) A study of chemical structure of soft and hardwood and wood polymers by FTIR spectroscopy. *J Appl Polym Sci* 71:1969–1975
34. Chiriac AP, Neamtu I, Nita LE, Nistor MT (2011) A study on the composites based on poly(succinimide)-*b*-poly(ethylene glycol) and ferrite and their magnetic response. *Composites* 42:1525–1531
35. Mustata F, Tudorachi N, Rosu D (2011) Curing and thermal behavior of resin matrix for composites based on epoxidized soybean oil/diglycidyl ether of bisphenol A. *Composites* 42:1803–1812
36. Salvador MA, Almeida P, Reis LV, Santos P (2009) Near-infrared delocalized cationic azo dyes. *Dyes Pigments* 82:118–123
37. Rayn C, Skibsted E, Bro R (2008) Near-infrared spectroscopy chemical imaging (NIR-CI) on pharmaceutical solid dosage forms. *J Pharm Biomed Anal* 48:554–561
38. Reich G (2005) Near-infrared spectroscopy and imaging: basic principles and pharmaceutical applications. *Adv Drug Deliv Rev* 57:1109–1143
39. Ciurczak EW, Drennen JK (2002) *Pharmaceutical and medical applications of near-infrared spectroscopy*. Marcel Dekker Inc, New York
40. Fernandez R, Blanco M, Galante MJ, Oyanguren PA, Mondragon I (2009) Polymerization of an epoxy resin modified with azobenzene groups monitored by near-infrared spectroscopy. *J Appl Polym Sci* 112:2999–3006
41. Furukawa T, Sato H, Shinzawa H, Noda I, Ochiai S (2007) Evaluation of homogeneity of binary blends of poly(3-hydroxybutyrate) and poly(L-lactic acid) studied by near infrared chemical imaging (NIRCI). *Anal Sci J* 23:871–876
42. Mijovic J, Andjeli S (1995) A study of reaction kinetics by near-infrared spectroscopy. 1. Comprehensive analysis of a model epoxy/amine system, *Macromol* 28:2787–2796